Optics and Spectroscopy, Vol. 85, No. 2, 1998, pp. 314–321. Translated from Optika i Spektroskopiya, Vol. 85, No. 2, 1998, pp. 338–346.
Original Russian Text Copyright © 1998 by Bespalov, Stasel'ko, Efimov, Krylov, Rebane, Erni, Ollikainen, Wild.

LASERS AND APPLICATIONS

Super-Regenerative SRS Amplification of Femtosecond Pulses in Compressed Hydrogen

V. G. Bespalov*, D. I. Stasel'ko*, Yu. N. Efimov*, V. N. Krylov*, A. Rebane**, D. Erni**, O. Ollikainen**, and U. Wild**

* *Vavilov State Optical Institute, All-Russia Scientific Center, St. Petersburg, 199034 Russia*

** *Laboratory of Physical Chemistry, Swiss Federal Institute of Technology, SN-8092 Zurich, Switzerland*

Received February 27, 1997

Abstract—An experimental study and numerical simulation of the amplification of femtosecond pulses on the basis of stimulated Raman scattering in compressed hydrogen were made. For pumping by 350-fs pulses with energy of 100 μJ of the second harmonic of radiation of a titanium-doped sapphire laser, the small-signal gain for 465-nm Stokes radiation separated out from the spectral continuum reached 10^{10}. The results of numerical calculations quantitatively and qualitatively agree with the experimental results for the pump energies lying below the threshold of spectral-continuum generation.

INTRODUCTION

The excitation of Stokes and anti-Stokes components in stimulated Raman scattering (SRS) in compressed gases is one of the most effective methods of frequency conversion for nano-, pico-, and femtosecond pulses [1–3]. Recent studies of SRS excitation in the femtosecond range of pulse durations showed a number of characteristic features of the process that are responsible for a decrease of its efficiency [3]. Among these are the following features: (1) a sharp enhancement of subsidiary nonlinear effects that are in competition with SRS, including the time and the spatial self-phase modulation of radiation pulses [4]; these processes deplete the pump because of the broadening of spatial–time spectra and the spectral-continuum generation [5]; they increase in importance because of a manyfold increase of the threshold power required for the excitation of nonstationary SRS by extremely short pulses; (2) the energy transfer from the Stokes wave to the pump wave [6] because of the phonon wave inertia; (3) a decrease of the effective length of SRS interaction because of a time delay of the pump pulse relative to the Stokes pulse; in the region of normal dispersion of gases, the delay reaches 1–20 fs/cm [7].

In the experiments [3] on SRS excitation in compressed hydrogen with femtosecond pulses of a titanium-doped sapphire laser with duration of 200 fs and wavelength of 780 nm, the authors did not manage to obtain efficient conversion (greater than 1%) in spite of variation of experimental parameters (cell length, hydrogen pressure, pump power, and excitation geometry) in a wide domain. In our opinion, this was caused primarily by the self-action of pump radiation, which caused the spectral-continuum generation in addition to the SRS excitation owing to the fact that these two processes had close thresholds. Indeed, a change made in [3] to pumping with pulses of the second harmonic (390 nm) of radiation of the same laser (in this case, the SRS threshold decreased by a factor of 10 and became considerably lower than the threshold of spectral-continuum generation), the efficiency of conversion to the first Stokes component sharply increased and reached 10–20%, all other experimental conditions being the same.

A change to the two-stage SRS conversion using the master oscillator–amplifier scheme considerably weakens the effect of the factors mentioned above. First, the presence of the input signal at the Stokes frequency whose intensity exceeds the level of spontaneous scattering causes a decreases of the pump power required to obtain a prescribed conversion efficiency. As a result, the effect of competing nonlinear effects is weakened. Moreover, according to [8], the use of an optimum delay between the Stokes pulse and the pump pulse enables one to decrease the effect of oscillatory energy exchange between them, which is typical of nonstationary SRS, and obtain the regime of super-regenerative amplification using above-threshold pump powers for self-excitation of SRS in a medium. Finally, the master oscillator–amplifier system has additional substantial advantages. It enables one to retain spatial and spectral characteristics of the input Stokes radiation and obtain bandwidth-limited pulses with supreme coherence [8], and, moreover sum several coherent pump beams and obtain a many-fold decrease of pulse duration [9]. Simultaneously, the energy fluctuations in the output beam are considerably minimized [10].

Note that the feasibility of discrimination between input pulses in spectrum and time is of no less importance than the feasibility of using SRS amplifiers for producing pulses with desired characteristics. Indeed, owing to both a large diversity of frequency shifts and

0030-400X/98/8502-0314$15.00 © 1998 МАИК Наука/Interperiodica Publishing

spectral widths in SRS amplification and the retention of amplitude and phase characteristics of the prime signal for gain levels of 10^3–10^9 [11], SRS amplifiers offer promise as efficient spectral–time active filters. Depending on the problem being solved, one can choose parameters of an SRS amplifier in a way providing its use either as a broad-band device, which is capable of amplifying input pulses with minimum distortions, or as a spectral–time discriminator, which separates out desired signals from broad-band noise. In the latter case, the SRS property of amplifying the Stokes signal only within the limits of a pump pulse when an SRS amplifier forms a sort of optical switch, the so-called time gate, is of considerable importance [12]. The energy characteristics of this switch and the feasibility of its use in optical tomography were studied in [13, 14] using an SRS amplifier on compressed hydrogen pumped with picosecond pulses.

One can form an input signal at the Stokes frequency using SRS oscillation in the same active medium [15] or additional radiation sources, such as tunable dye lasers [16] and semiconductor lasers [17]. In the present work, we formed the input Stokes signal using the spectral-continuum generation [18]. This relatively new and universal method makes it possible to form signals in the IR, visible, and UV spectral regions.

In what follows, we present the results of our studies of SRS amplification in compressed hydrogen pumped by femtosecond pulses of the second harmonic of radiation of a titanium-doped sapphire laser. Our aim was to estimate the feasibility of increasing efficiency of SRS conversion and the potentialities of using nonstationary SRS for spectral–time selection and amplification of weak signals.

EXPERIMENTAL SETUP

The schematic diagram of the experimental setup is presented in Fig. 1. A CPA-1 laser system produced by the Clark-MXR company and operating on sapphire crystals doped with titanium ions was used as a radiation source. It consisted of a master oscillator producing femtosecond pulses, a system forming lengthened chirped pulses, a regenerative amplifier, and an output compressor on the basis of a diffraction grating [19]. The duration of output pulses at half maximum at the wavelength $\lambda = 780$ nm was 200 fs. A separate pulse had an energy of 0.75 mJ, with the pulse repetition frequency being equal to 1 kHz. The SRS amplifier was pumped by pulses of the second harmonic ($\lambda_p = 390$ nm) generated in a KDP crystal 2.5 mm thick. The SHG increased their duration up to 400 fs, and the energy of pump pulses reached the value $W_p = 0.3$ mJ. It could be varied with the help of a special filter F with a variable transmission, which hold constant the direction of propagation of an attenuated beam. The SRS amplifier represented a cell C 100 cm long. The cell was made of stainless steel, had an aperture of 25 mm, and was filled with hydrogen at a pressure of 45 atm. The dephasing

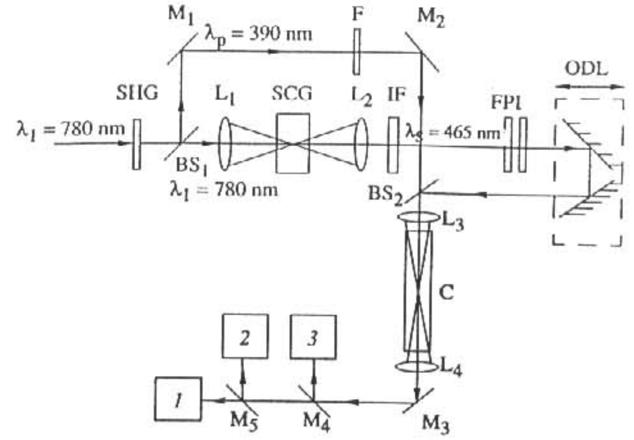

Fig. 1. Schematic diagram of the experimental setup. (SHG) nonlinear crystal for second-harmonic generation, (SCG) generator of the spectral continuum, (IF) interference filter, (F) filter with controllable transmission, (FPI) Fabry–Perot interferometer forming a train of damping signal pulses, (ODL) optical delay line, (C) cell with compressed hydrogen, (*1*) energy meters, (*2*) system for measuring the pulse duration, (*3*) system for measuring the radiation spectrum, (M_1–M_5) dielectric mirrors, (BS_1, BS_2) beam splitters, (L_1–L_4) lenses.

time of molecular vibrations in hydrogen at this pressure is $T_2 = 140$ ps [20]. It is large in comparison with the pump pulse duration, which determined the strongly nonstationary nature of amplification.

To form an input signal at the Stokes frequency, we used the radiation at the fundamental frequency transmitted through the KDP crystal and a dichroic mirror D_1. This radiation was focused by a lens L_1 into a glass plate used for the spectral-continuum generation (SCG). The spectral continuum excited in glass was collimated by a lens L_2. The desired portion of the spectrum in the blue region near the Stokes wavelength of 465 nm was separated out by an interference filter IF. It had a half-width of 8 nm (370 cm^{-1}). The duration of signal pulses at the Stokes frequency was approximately equal to the duration of the corresponding pump pulses (~200 fs) [21], and their energy at the cell input was 10^{-6} μJ. On passing through the Fabry–Perot interferometer FPI, which formed a train of damping femtosecond pulses, and a controllable optical delay line ODL, the signal beam was made spatially coincident with the pump beam and focused by a lens with a focal length of 100 cm to the center of the SRS cell. The use of the optical delay line and the train former considerably increased the productive capacity of the measurements and their reproducibility. Moreover, it provided the optimization of the major parameters of the SRS amplifier (the input signal gain, the output energy of the Stokes pulse, and the Stokes pulse duration). For this purpose, the dependence of gain on the pump energy, the input pulse energy, and the time delay between the input pump pulses and the Stokes signal was studied. The Stokes radiation emerging from the SRS cell was

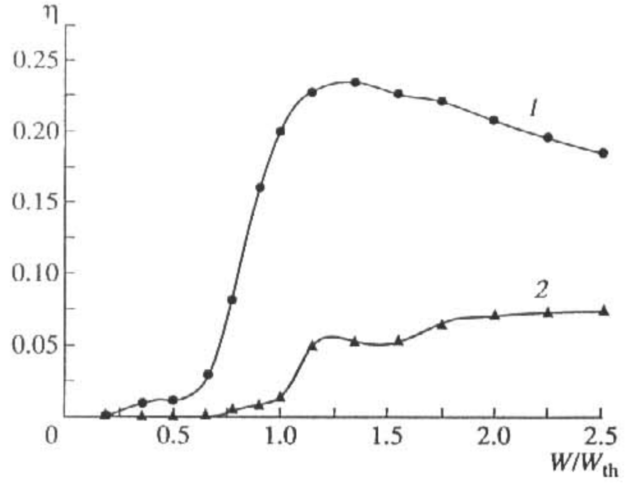

Fig. 2. Experimental dependences of the conversion efficiency η on the pump energy reduced to the self-excitation threshold W_{th} for (*1*) SRS amplification and (2) SRS oscillation.

collimated and entered units for measuring energy, spectrum, and pulse duration. The energy (power) was measured with calorimeters, the spectrum was measured with prism and diffraction spectrographs, and the pulse duration was estimated using cross- and autocorrelation systems on the basis of noncollinear second- and third-harmonic generation in a BBO crystal 1 mm thick.

EXPERIMENTAL RESULTS

At the first stage of experiments, we measured the dependences of the output energy of the first Stokes component on the pump energy in the range of 10–100 μJ for a fixed energy of the input Stokes signal (10^{-6} μJ). The delay between the pump pulse and the input signal was chosen in a way providing the maximum signal at the output of the SRS amplifier in the absence of the Fabry–Perot interferometer. Figure 2 presents the dependence of the energy efficiency of SRS conversion η (it is defined as the ratio of output energy of Stokes radiation to the input pump energy) on the input pump energy (curve *1*) and a similar dependence for the case of SRS oscillation without an input signal under the same experimental conditions (curve 2). For the given level of the input signal, the highest amplification efficiency was obtained in the super-regenerative regime, i.e., in the case where the pump energy exceeded the threshold of SRS self-excitation starting with spontaneous noise. One can see from Fig. 2 that the use of an external Stokes signal decreases by a factor of 1.5–3 the pump energy required for obtaining a prescribed conversion efficiency. Moreover, it increases the maximum value of η by a factor of more than three (up to 25%). Efficient SRS amplification is obtained for the pump energies above 15 μJ. The output signal sharply increases for the energies exceeding 25 μJ, and its growth becomes considerably slower for the pump energies in the range of 50–100 μJ. It is likely that the slowing down was associated with the spectral-continuum generation [3, 4], which was in competition with the SRS and depleted the pump. The threshold of this process in our experiments was about 50 μJ. The gain, which was defined as the ratio of the output Stokes energy to the input signal energy, reached 1.5×10^7 for the input pump energy of 100 μJ. Note that the SRS amplification provided a considerable improvement of reproducibility of the output Stokes energy from pulse to pulse. Moreover, the spatial structure of the Stokes beam became considerably more smooth and contained no sharp random amplitude spikes in the beam cross section, which are typical of SRS oscillation.

At the second stage, we studied in detail the dependence of SRS gain on the energy of the prime pulse and its delay relative to the pump pulse. For this purpose, the Stokes signal was passed through the Fabry–Perot amplifier with a spacing of 430 μm. The reflectivity of its mirrors at the wavelength of Stokes radiation was equal to 50%. The etalon formed a train of 200-fs signal pulses with a time interval of 2.9 ps. Each subsequent pulse was four times weaker than the preceding one. Controlling the optical delay line at the output of the interferometer, we could successively make the pump pulse coincident in time with eight signal pulses of the train with energies decreasing from 10^{-6} to 10^{-10} μJ. As a result, we obtained in one experiment the dependences of the output energy of amplified Stokes pulses on both the time delay between the pulses and the input energy for different values of the pump energy. Figure 3 illustrates examples of these dependences (a) for the input pump energy of 27 μJ lying below the threshold of SRS self-excitation, which is equal to 37 μJ, and (b) for the pump energy of 60 μJ, i.e., in the super-regenerative regime. These and similar experimental curves were used to plot the dependences presented in Fig. 4. They describe gain as a function of energy of the input Stokes signal for different pump energies. For the input signal energy of 10^{-6} μJ, gain ranged from 5×10^5 (η = 2.5%) to 1.58×10^7 (η = 16%). For the input energy of 10^{-10} μJ, it reached 3×10^{10} (η = 1%).

Let us calculate the number of photons in the signal beam that is required to obtain an amplified Stokes signal whose energy exceeds the SRS energy in the super-regenerative regime. One can see from the experimental results (Fig. 3) that the level of the amplified Stokes signal becomes comparable with the level of the signal obtained in the super-regenerative regime for the eighth pulse of a train. In this case, the energy of the input Stokes signal is $(1/4)^7 \times 10^{-6}$ μJ = 6×10^{-11} μJ, which corresponds to approximately 70 photons (the energy of a Stokes photon is $W = 9 \times 10^{-13}$ μJ). For the seventh or the sixth pulse of a train, the amplified Stokes signal, as a rule, was noticeably stronger than the signal obtained in the super-regenerative SRS regime. This corresponded to 280–1120 Stokes photons at the input. Starting from the experimental data on the threshold of

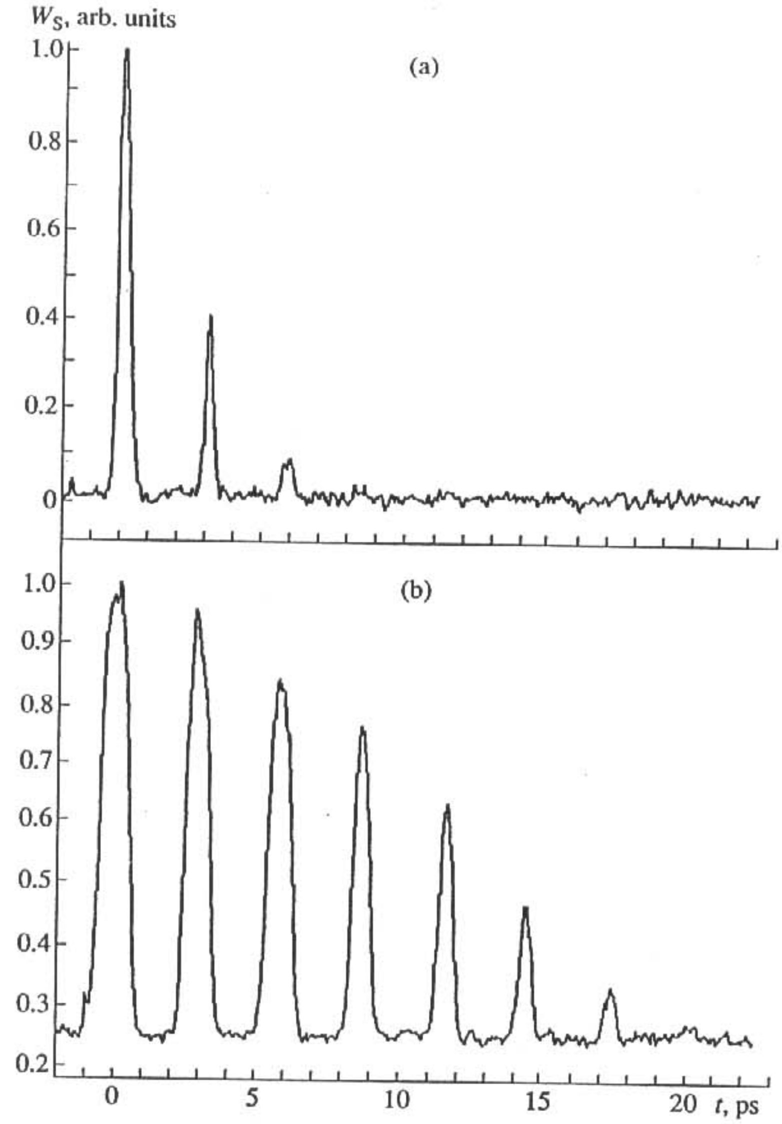

Fig. 3. Experimental dependence of the output Stokes energy W_S on the time delay t between the pump pulse and the train of damping signal pulses. W_p = (a) 27 and (b) 60 μJ.

SRS in the super-regenerative regime, one can estimate the number of spontaneous Stokes photons produced in the medium. According to [13], at the threshold of nonstationary SRS with conversion efficiency as large as 1%, gain is equal to e^{23} or 10^{10}. Taking into account the fact that the threshold pump energy is equal to 37 μJ and the Stokes signal produced in this case has an energy of 0.37 μJ, we find that the number of spontaneous photons produced for pump energies of 37–100 μJ is equal to 40–100. The relationship between the number of signal photons injected into the medium and the number of spontaneous photons at the self-excitation threshold is in quantitative agreement with the results of [10], where the authors observed the suppression of the spontaneous nature of the regime of nonstationary SRS amplification under conditions where this ratio was exceeded by a factor of ten. Note that the number of spatial–time modes formed in the SRS process and determining the number of photons required for the suppression of spontaneous scattering is proportional to the product of spectral width of the pump signal by its duration and to the number of diffraction-limited channels formed by the pump beam. Taking into account that the pump pulses used in the experiments were not bandwidth-limited and the pump beam divergence was 3–4 times greater than the diffraction value, it may be concluded that the characteristics obtained by us are different from the limiting values and can be improved by approximately an order of magnitude by way of optimizing parameters of the pump laser.

The dependences presented in Figs. 3a and 3b and similar dependences for other W_p suggest that the half-width of the time gate of the SRS amplifier substantially depends on both the pump energy and the input

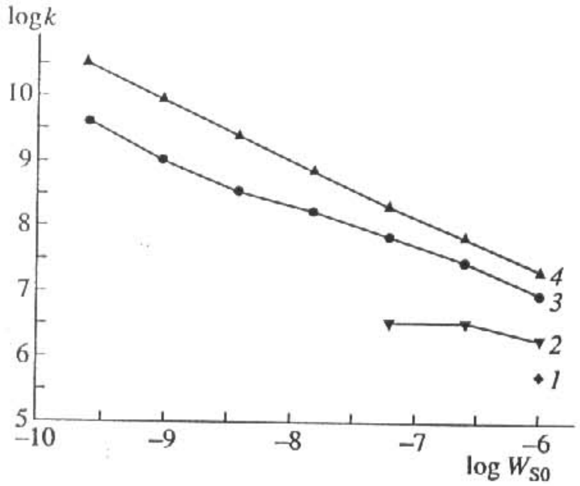

Fig. 4. Dependence of the SRS gain on the level of the input Stokes signal for W_p = (*1*) 20, (*2*) 27, (*3*) 40, and (*4*) 100 μJ.

signal energy. For the fixed energy of the input signal $W_{S0} = 10^{-6}$, it increases from 350–400 to 800–900 fs with increasing the pump energy from 20 to 100 μJ. Moreover, it noticeably decreased with decreasing input signal energy. A detailed analysis of these dependences, as well as time and spectral characteristics of the amplified Stokes pulses, will be presented elsewhere.

NUMERICAL SIMULATION AND ANALYSIS

To determine the highest efficiencies attainable for the SRS conversion of femtosecond pulses and the optimum relationships between the input signal and the pump in the regimes of super-regenerative amplification, we carried out numerical simulation of nonstationary SRS oscillation and amplification of signal pulses propagating in the same direction as pump pulses for the parameters close to those used in our experiments.

In media with a homogeneously broadened line of spontaneous Raman scattering, these processes are commonly described in the approximation of slowly varying amplitudes by the system of coupled differential equations for the complex amplitudes of plane pump, Stokes, and phonon waves (specified by the subscripts p, S, and ph, respectively)

$$E_{p,S,ph}(z,t) = \frac{1}{2}(A_{p,S,ph}\exp[i\{k_{p,S,ph}z - \omega_{p,S,ph}t\}] + \text{c.c.}). \quad (1)$$

Here, A_p, A_S, A_{ph}, $\omega_{p,S,ph}$, and $k_{p,S,ph}$ are the complex amplitudes, the frequencies, and the wave vectors of the interacting waves [22]. Neglect of subsidiary nonlinear processes, the excitation of higher Stokes and anti-Stokes components, the change of the difference of populations for the initial and final levels, and quantum noise [23], substantially simplifies the system and reduces it to the form

$$\left[\frac{\partial}{\partial z} + \frac{1}{V_p}\frac{\partial}{\partial t}\right]A_p = -ik_1\left(\frac{\omega_p}{\omega_S}\right)A_S A_{ph}, \quad (2a)$$

$$\left[\frac{\partial}{\partial z} + \frac{1}{V_S}\frac{\partial}{\partial t}\right]A_S = ik_1 A_p A_{ph}^*, \quad (2b)$$

$$\left[\frac{\partial}{\partial t} + \frac{1}{T_2}\right]A_{ph} = ik_2 A_p A_S^*, \quad (2c)$$

where $k_1 = 2\pi N(\frac{\partial\alpha}{\partial Q})$ and $k_2 = \frac{N}{2\omega_{ph}}(\frac{\partial\alpha}{\partial Q})$ are the coupling constants, N is the density of molecules on the initial level, $(\partial\alpha/\partial Q)$ is the derivative of polarizability with respect to the vibrational coordinate, $V_{p,S} = c/n_{p,S}$ are the group velocities of waves, c is the speed of light in vacuum, $n_{p,S}$ are the refractive indices for the wavelengths of pump and Stokes signals, and T_2 is the dephasing time of molecular vibrations.

In the case of a given pump and a medium without dispersion, system (2) has an analytical solution [22]. In the case where the efficiency of pump conversion to the Stokes wave exceeds 1% and a medium possesses dispersion, one should solve system (2) by numerical methods [6].

To solve the system numerically, we rename the variables and reduce the constants k_1 and k_2 to the quantity measured in the experiment, namely, the gain g (cm/W) of stationary SRS. These changes are made in accordance with [24] and give

$$\left[\frac{\partial}{\partial z} + \frac{1}{V_p}\frac{\partial}{\partial t}\right]e_p = -g\left(\frac{\omega_p}{\omega_S}\right)\frac{e_S q}{2}, \quad (3a)$$

$$\left[\frac{\partial}{\partial z} + \frac{1}{V_S}\frac{\partial}{\partial t}\right]e_c = g\frac{e_p q^*}{2}, \quad (3b)$$

$$\left[\frac{\partial}{\partial t} + \frac{1}{T_2}\right]q = \frac{e_S^* e_p}{T_2}, \quad (3c)$$

where $|e_{p,S}|^2 = \frac{1}{2}\varepsilon_0 c|E_{p,S}|^2 = I_{p,S}$, $q = \frac{1}{2}\varepsilon_0 c\frac{A_{ph}}{T_2 k_2}$, $g = \frac{4\omega_c k_1 k_2 T_2}{\varepsilon_0 c}$, ε_0 is the dielectric constant, and $I_{p,S}$ is the power density for the pump or Stokes waves (in W/cm^2).

Equations (3) were solved numerically using the initial conditions corresponding to the experiment. They had the form

$$|e_p(0,t)|^2 = I_{p0}\exp\left[-\left(\frac{t-t_p}{\tau_p}\right)^2\right], \quad (4a)$$

$$|e_S(0,t)|^2 = I_{S0}\exp\left[-\left(\frac{t-t_p-t_d}{\tau_S}\right)^2\right] + |e_p(0,t)|^2\exp(-23), \quad (4b)$$

$$q(0,t) = 0, \quad (4c)$$

where I_{p0} and I_{S0} are the maximum intensities of the pump and the input Stokes signal, $2\tau_{p,S}$ are the durations of these pulses at a level of e^{-1}, $t_p = 5\ln(2)\tau_p$, and τ_d is the time delay of the pump pulse peak with respect to the peak of the input Stokes pulse. The second term on the right-hand side of equation (4b) corresponds to the level of averaged intensity of spontaneous Raman scattering. According to the experimental conditions, we used the following values of input parameters: τ_p = 140 fs, τ_S = 70 fs, T_2 = 140 ps, and I_{p0} = 2–250 GW/cm^2 or e_p = 1.5–15 (GW/cm^2)$^{1/2}$ (see the Appendix).

System (3) was solved by the Runge–Kutta method of second order with the time step $\Delta\tau$ = 2 fs and the spatial step Δz = 0.1 cm. We used 1000 time points and 1000 spatial points. To take into account the group velocities of Stokes and pump waves whose difference in our conditions was characterized by a delay of 2 fs/cm, we used the following procedure. System (3) was solved without account of group velocities, in the moving coordinate system with $\tau' = t - z/c$ and $z' = z$. At each step corresponding to the spatial coordinates $z = \Delta z, 2\Delta z, \ldots$, we determined the functions $e_{p,S}(t, \Delta z)$, $e_{p,S}(t, 2\Delta z)$, etc. At the tenth step corresponding to z = 1 cm, the function $e_S(t, 10\Delta z)$ was shifted by one time step corresponding to 2 fs, i.e., we set $e_S(t, 10\Delta z) = e_S(t - \Delta t, 10\Delta z)$, and the calculation was continued till the point $z = 20\Delta z$, where we performed a similar procedure, and so on.

From the calculations it follows that one should considerably shift the input Stokes signal forward in time with respect to the pump pulse at the input of the SRS amplifier to obtain efficient SRS amplification of femtosecond pulses. A similar conclusion has been made by us earlier in the study of super-regenerative nonstationary SRS amplification using nanosecond pump pulses [8]. The optimum time shift changed from 200 to 350 fs with increasing pump power (Fig. 5). This is attributed to the fact that the highest efficiency of energy transfer from the pump wave to the Stokes wave is obtained in the region corresponding to the peak of the phonon wave which, in view of inertia of the medium, corresponds to the trailing edge of the pump wave. Because of this, the Stokes signal entering the amplifier ahead of the pump pulse provides a spatial–time shift of the phonon wave peak toward the peak of the pump pulse, i.e., the region where the efficiency of interaction of the beams is the highest, which increases the efficiency of SRS conversion.

Figure 6 illustrates the calculations of conversion efficiency as a function of pump energy at the input of the cell for the SRS amplification of the Stokes signal with the optimum shift and the energies W_{S0} = (2) 10^{-6},

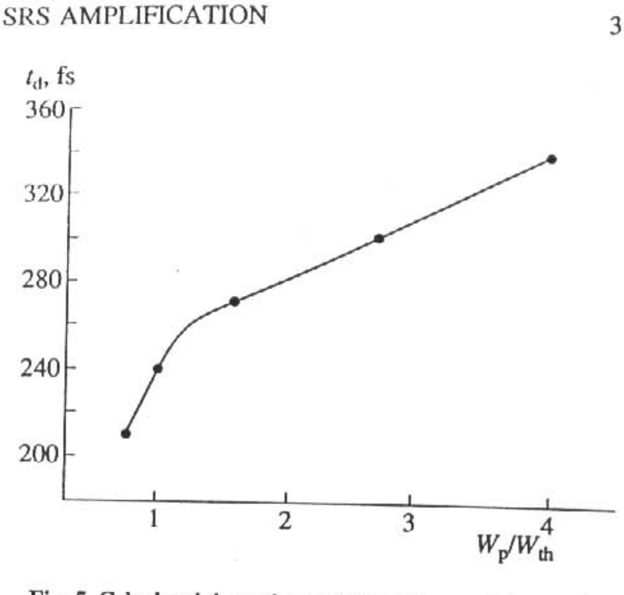

Fig. 5. Calculated dependence of the optimum delay on the input pump power.

(3) 10^{-4}, and (4) 10^{-2} μJ. Curve 1 presents the conversion efficiency for the SRS oscillation developed from the level of spontaneous noise. The calculations were made for the pump energies up to twice the threshold of SRS self-excitation. This limitation was caused by the spectral-continuum generation that was observed in the experiments for higher pump energies, but was not taken into account in the calculations. One can see from the curves that the SRS amplification gives a higher efficiency and the pump threshold for W_{S0} = 10^{-6} μJ is two times lower than the pump threshold for self-excitation, which agrees with the experimental results (Fig. 2). As the input signal increases by four orders of magnitude (W_{S0} = 10^{-2} μJ), the threshold pump energy becomes ten times lower and the conversion efficiency increases by a factor of 1.5. This fact specifies natural boundaries between the use of different methods of Stokes signal formation and is helpful in the development of SRS amplifiers of the femtosecond range. The use of the spectral continuum is characterized by the simplicity of signal beam formation and the universality. However, it is impossible to build up in this case a sufficiently strong input Stokes signal providing a high conversion efficiency. On the other hand, a conventional scheme using an additional master SRS oscillator adds complexity to the experimental setup, but, in view of the results presented above, offers possibilities of a strong increase of η and decrease of requirements for the pump energy owing to considerably higher values of Stokes signal energy.

All the curves in Fig. 6 have typical regions of efficiency increase and decay. The analysis of the time dependences of the Stokes signal intensity and the pump intensity for different levels of the latter suggests that the decay is associated with the reverse energy transfer from the Stokes signal to the pump pulse. For the pump intensity close the threshold (point a in Fig. 6),

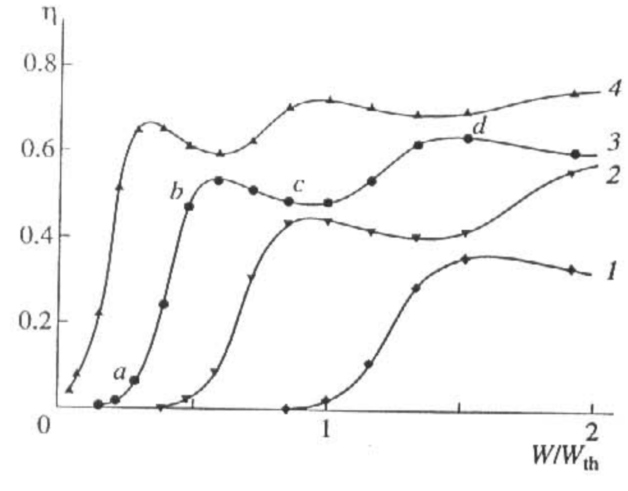

Fig. 6. Calculated dependences of the conversion efficiency on the pump energy reduced to the self-excitation threshold W_p for (1) SRS oscillation and (2–4) SRS amplification for W_{S0} = (2) 10^{-6}, (3) 10^{-4}, and (4) 10^{-2} μJ.

a single Stokes pulse delayed by approximately 200 fs with respect to the peak of the pump signal is formed. As the pump increases, the intensity of the Stokes pulse increases as well and, above a certain pump level, this pulse completely depletes it at the trailing edge. Because of the inertia of the phonon wave, its amplitude does not vanish simultaneously with the pump, which initiates the reverse energy transfer from the Stokes pulse to the pump (point *b* in Fig. 6), with the phase of the regenerated pump wave being changed by π [24]. Simultaneously, the process of direct energy transfer from the pump to the Stokes pulse at the leading edge of this pulse is developed. It is favored by the shift of the Stokes pulse toward the beginning of the pump pulse because of the dispersion of their group velocities. This process is accompanied by sharpening of the time profile of the Stokes pulse and its shortening down to 100 fs, which agrees with the results of [3], where the authors observed shortening of the Stokes pulse down to 130 fs, with the pump pulse duration being equal to 400 fs. Further on, the phonon wave at the trailing edge of the Stokes pulse decays to the zero level, and subsequently its phase changes by π (because the phases of the Stokes wave and the regenerated portion of the pump wave differ by π), which causes the energy transfer from the regenerated portion of the pump to the Stokes wave and the formation of the second Stokes subpulse (point *c* in Fig. 6). The first Stokes pulse travels with a higher velocity than the pump pulse, "eats out" an undepleted portion of the leading edge of the pump, and increases in amplitude. Further on, the second Stokes subpulse depletes the regenerated pump, the reverse process proceeds and takes the form of energy transfer from the second Stokes subpulse, the third Stokes subpulse is formed in an undepleted pump (point *d* in Fig. 6), etc. As the pump intensity increases, the Stokes pulses have a general tendency to become narrower and shift toward the beginning of the pump pulse.

It is evident that the reverse conversion of the Stokes wave to the pump wave slows down an increase of the energy of Stokes radiation and causes a nonmonotonic increase of conversion efficiency (Fig. 6). This process qualitatively shows itself in the experiment. In particular, one can clearly see from curve *2* in Fig. 2, which corresponds to the SRS oscillation developed from spontaneous noise, that an initial sharp increase of conversion efficiency subsequently slows down. A similar curve *1*, which is plotted for SRS amplification, is characterized by a nonmonotonic variation of η as well. However, this behavior may be caused to a large extent by the spectral-continuum generation, which depletes the pump and was observed for the pump energies above 50 μJ, but was not taken into account in our calculations [25]. To obtain a better agreement of the simulation results with the experimental data, one should take into account the spatial effects associated with the difference of structures of the Stokes beams being amplified and the pump beams. They are taken into account in addition to the self-action effects, which are described by the terms introduced into the equations.

CONCLUSIONS

The results of our studies clearly show that the SRS amplification offers promise for the extension of the frequency range in which femtosecond pulses are generated and an increase of the efficiency of their conversion. Of particular interest is the super-regenerative amplification. The employment of this regime gave gain as high as 3×10^{10}, which exceeds the values obtained in the self-excitation regime. An original scheme proposed by us for obtaining a delay of the pump pulse relative to a train of damping signal pulses can be used for rapid determination and optimization of the major parameters of SRS amplification. The calculations that were made taking into account the dispersion of group velocities of pump and Stokes waves qualitatively and quantitatively agree with the experimental results obtained in the region of pump energies where the effect of subsidiary nonlinear processes may be neglected. The calculations show the ways of increasing SRS conversion efficiency and offer promise for a further optimization of tunable sources of femtosecond pulses designed on the basis of SRS amplification. Recommendations concerning the use of various methods of generation of input Stokes pulses are formulated.

ACKNOWLEDGMENTS

This work was supported by the Russian Foundation for Basic Research (project no. 97-02-18380) and the Russian State Program on Fundamental Metrology. It was carried out within the framework of collaboration with the countries of Central and Eastern Europe that was supported by the Federal Department of Foreign Affairs of Switzerland under the direction of the National Scientific Center of Switzerland.

APPENDIX

One can use the expression for the increment of nonstationary SRS [22]

$$G_p \sim \left[\int_{-\infty}^{\infty}\int_{0}^{L} I_p(t, z)dtdz\right]^{1/2}, \quad (5)$$

to obtain a relation between the excitation of SRS by a plane pump beam with intensity $I_p(t)$ in a cell of length L and the excitation of SRS by a diffraction-limited pump beam with energy W_p that is focused by a lens with $F = L/2$ into a cell of length L. Taking into account that focusing gives $I_p(z) = P[(1 - z/F)^2 + z^2/(k_p a^2)^2]^2$, where P is the beam power and a is the beam radius, one can obtain

$$\left[\int_{-\infty}^{\infty}\int_{0}^{L} I_p(t, z)dtdz\right] = \frac{2\pi W_p}{\lambda_p}, \quad (6)$$

where λ_p is the pump wavelength. In the case of SRS excited by plane beams with the Gaussian time dependence of intensity of form (4a), we have

$$\left[\int_{-\infty}^{\infty}\int_{0}^{L} I_p(t, z)dtdz\right] = \sqrt{\pi} I_{p0}\tau_p L. \quad (7)$$

Equating (6) and (7), we obtain

$$W_p = \frac{\lambda L \tau_p I_{p0}}{2\sqrt{\pi}}, \quad I_{p0} = \frac{2\sqrt{\pi} W_p}{\lambda L \tau_p}. \quad (8)$$

REFERENCES

1. Bespalov, V.G., Krylov, V.N., Mikhailov, V.N., Parfenov, V.A., and Stasel'ko, D.I., *Opt. Spektrosk.*, 1991, vol. 70, no. 2, pp. 193–196.
2. Everall, N.J., Partanen, J.P., Barr, J.R.M., and Shaw, M.J., *Opt. Commun.*, 1987, vol. 64, no. 4, pp. 393–397.
3. Krylov, V., Rebane, A., Ollikainen, O., Erni, D., Wild, U., Bespalov, V., and Staselko, D., *Opt. Lett.*, 1996, vol. 21, no. 6, pp. 381–383.
4. Wang, J., Siegel, Y., Lii, C., Mazur, E., and Reintjes, J., *J. Opt. Soc. Am. B: Opt. Phys.*, 1994, vol. 11, no. 6, pp. 1031–1037.
5. *Supercontinuum Laser Source*, Alfano, R.R., Ed., New York: Springer, 1989.
6. Hilfer, G. and Menyuk, C.R., *J. Opt. Soc. Am. B: Opt. Phys.*, 1990, vol. 7, no. 5, pp. 739–749.
7. Akhmanov, S.A., Chirkin, A.S., and Drabovich, K.N., *IEEE J. Quantum Electron.*, 1968, vol. 4, no. 3, pp. 598–608.
8. Bespalov, V.G., Krylov, V.N., Stasel'ko, D.I., Sizov, V.N., Parfenov, V.A., and Yutanova, E.Yu., *Opt. Spektrosk.*, 1987, vol. 63, no. 6, pp. 1253–1260.
9. Ewing, J.J., Haas, R.A., Swingle, J.C., George, E.V., and Krupke, W.F., *IEEE J. Quantum Electron.*, 1979, vol. 15, no. 5, pp. 368–379.
10. Duncan, M.D., Mahón, R., Tankersley, L.L., and Reintjes, J., *J. Opt. Soc. Am. B: Opt. Phys.*, 1990, vol. 7, no. 7, pp. 1336–1345.
11. Duncan, M.D., Mahon, R., Tankersley, L.L., Hilfer, G., and Reintjes, J., *J. Opt. Soc. Am. B: Opt. Phys.*, 1990, vol. 7, no. 2, pp. 202–210.
12. Duncan, M.D., Mahon, R., Tandersley, L.L., and Reintjes, J., *Opt. Lett.*, 1991, vol. 16, no. 23, pp. 1868–1870.
13. Duncan, M.D., Mahon, R., Tandersley, L.L., and Reintjes, J., *J. Opt. Soc. Am. B: Opt. Phys.*, 1988, vol. 5, no. 1, pp. 37–52.
14. Moon, J.A., Mahon, R., Duncan, M.D., and Reintjes, J., *Opt. Lett.*, 1994, vol. 19, no. 16, pp. 1234–1236.
15. Grasyuk A.Z., *Trudy Fiz. Inst. im. P.N. Lebedeva Akad. Nauk SSSR*, 1974, vol. 76, pp. 75–115.
16. Gomes, A.S.L. and Lawandy, N.M., *Opt. Lett.*, 1994, vol. 19, no. 6, pp. 408–410.
17. Wessel, J.G., Repasky, K.S., and Carlsten, J.L., *Proc. SPIE–Int. Soc. Opt. Eng.*, 1996, vol. 2700, pp. 398–408.
18. Selker, M.D. and Lawandy, N.M., *Electron. Lett.*, 1990, vol. 26, no. 6, pp. 409–410.
19. Krylov, V., Rebane, A., Kalintsev, A., Schwoerer, H., and Wild, U.P., *Opt. Lett.*, 1995, vol. 20, no. 2, pp. 198–200.
20. Murray, J.R. and Javan, A., *J. Mol. Spectrosc.*, 1972, vol. 42, no. 1, pp. 1–26.
21. Nishioka, H., Odajima, W., Ueda, K., and Takuma, H., *Opt. Lett.*, 1995, vol. 20, no. 24, pp. 2505–2507.
22. Carman, R.L., Shimizu, F., Wang, C.S., and Bloenbergen, N., *Phys. Rev. A*, 1970, vol. 2, no. 1, pp. 60–72.
23. Englund, J.C. and Bowden, C.M., *Phys. Rev. A*, 1990, vol. 42, no. 5, pp. 2870–2889.
24. George, S.M. and Harris, C.B., *Phys. Rev. A*, 1983, vol. 28, no. 2, pp. 863–878.
25. Mikheev, P.M., Djidjoev, M.S., Platonenko, V.T., and Savil'ev, A.B., *Proc. SPIE–Int. Soc. Opt. Eng.*, 1996, vol. 2778, pp. 860–861.

Translated by A. Kirkin